

Showers in Lead Produced by Electrons with Energies from 300 MeV to 1 BeV*

H. THOM

Laboratory of Nuclear Studies, Cornell University, Ithaca, New York

(Received 12 March 1964)

The behavior of electron-initiated showers in a lead-plate expansion cloud chamber has been measured for primary energies of 277, 528, 845, and 990 MeV, in terms of the secondary electrons with angles within about 60 deg of the shower axis. Empirical formulas are derived from the experimental data, for characteristic average shower quantities as functions of primary energy. The track length, for example, follows a relation of the form $L_T = 0.073E_0^{0.92}$ radiation lengths, where E_0 is measured in MeV. Expected standard errors in determining energies of individual showers by measuring the various quantities are also given. A new tabulation of the results of Wilson's Monte Carlo calculations is given for primary electrons and photons with energies from 50 to 300 MeV. The average numbers of electrons with energies greater than 8 and 10 MeV given in this paper correct the originally published curves and are in good agreement with the results of Crawford and Messel. Approximate comparison is made between the experimentally measured shower behavior and the calculated behavior, and good agreement is found.

I. INTRODUCTION

THE purpose of this paper is to present data on electron-shower development as observed in a lead-plate cloud chamber so as to provide empirical quantitative information on shower behavior as a function of primary electron energy. No attempt is made to draw theoretical conclusions. A part of the paper will be taken up with listing corrections to an earlier "Monte Carlo Study of Shower Development" by Wilson.¹ It has been found that some of the numerical results listed in that paper were inconsistent with the raw data as given by the shower "histories." The new numbers which are given here are only those which can be obtained directly from the original histories, and do not include any calculation. Some general comparisons will be made between the experimentally measured shower behavior and a model of expected behavior suggested by Wilson.

Section II of this paper explains the experimental and scanning procedures by which the experimental results were obtained; the third section contains exact definitions of the quantities measured and presents the experimental data. Section IV contains tables of Wilson's calculations which have been rechecked; it also contains a brief comparison of these values with the recent calculations of Crawford and Messel.² In Sec. V an approximate procedure is discussed by which the calculations of Wilson can be compared with the experimental numbers, and this comparison is made for the average number of electrons as a function of thickness of lead in showers initiated by 300-MeV electrons. A discussion of the experimental results on average shower behavior is given in Sec. VI and occasional reference is made to analogous calculated results. In Sec. VII shower fluctuations are discussed; a table is given which determines the expected standard error within which the energy of any particular shower can be determined by measuring the various quantities discussed in Sec. VI.

II. EXPERIMENTAL AND SCANNING PROCEDURES

The external photon beam of the Cornell synchrotron passed through a 5-mil Cu target located at the front edge of an analyzing magnet. Electrons of the appropriate primary energy, produced in the target, were deflected into an expansion cloud chamber. The cloud chamber had an observable volume of 11 in. diam in the horizontal plane, and 3.5-in. depth. Nine lead plates, 7.5-in. wide by 3.5-in. deep, were placed in the chamber with about $\frac{3}{4}$ in. separation between them. The first plate was $\frac{1}{2}$ radiation length (r.l.) thick (0.20 in. = 1 r.l.), the last was 2 r.l. and the other seven were of 1-r.l. thickness. Thus, the gaps, in which the shower development could be observed, occurred at 0, $\frac{1}{2}$, $1\frac{1}{2}$, $2\frac{1}{2}$, \dots , $7\frac{1}{2}$, and $9\frac{1}{2}$ r.l. Primary electrons upon entering the chamber passed through less than 0.1 r.l. of glass, which has been ignored in the following analysis. Stereoscopic photographs were taken with an 8-deg angular divergence, and on the average two to three showers were seen in each photograph.

The energy E_0 of the electrons incident on the chamber was determined by wire measurements. Showers were studied in four different energy intervals, within each of which the number of showers as a function of primary energy was essentially constant. The half-width $\Delta E_0/E_0$ in each case was about $\pm 9\%$, and possible systematic errors in evaluating the energy are estimated to be $\leq \pm 4\%$.

The showers were analyzed in such a way as to discriminate against low-energy secondary electrons and background. The criteria by which tracks were disregarded were: if they had a projected angle of greater than 60° to the shower axis; if they were appreciably gas-scattered or heavily ionizing; if they left the chamber through the top or bottom faces; or if they originated far from the main body of the shower. In effect the projected-angle criterion and the requirement that the track must stay within the chamber, together amounted to counting tracks which had no more than about 60-deg polar angle with respect to the direction of the shower axis.

* Work supported in part by the U. S. Office of Naval Research.

¹ R. R. Wilson, Phys. Rev. **86**, 261 (1952).

² D. F. Crawford and H. Messel, Phys. Rev. **128**, 2352 (1962).

TABLE I. Experimental results: the probability of observing N electrons as a function of shower depth t and primary electron energy E_0 . (Statistical error in the probability P is $\Delta P = \pm [P(1-P)/m]^{1/2}$ where m is the number of showers observed.) The last two rows give the average number of electrons and the variance of the number at each value of thickness. ΔE_0 is the half-width of the primary energy dispersion.

t (r.l.) $N \setminus$		$E_0=990$ MeV; $m=201$ showers; $\Delta E_0=85$ MeV								
		$\frac{1}{2}$	$1\frac{1}{2}$	$2\frac{1}{2}$	$3\frac{1}{2}$	$4\frac{1}{2}$	$5\frac{1}{2}$	$6\frac{1}{2}$	$7\frac{1}{2}$	$9\frac{1}{2}$
0		0.015	0.020	0.025	0.015	0.020	0.070	0.080	0.154	0.378
1		0.642	0.154	0.070	0.050	0.070	0.055	0.114	0.189	0.229
2		0.184	0.194	0.095	0.080	0.065	0.114	0.179	0.229	0.249
3		0.129	0.199	0.139	0.104	0.099	0.104	0.139	0.139	0.070
4		0.030	0.149	0.154	0.164	0.134	0.159	0.154	0.104	0.030
5			0.114	0.124	0.134	0.189	0.154	0.119	0.089	0.035
6			0.095	0.134	0.169	0.144	0.109	0.080	0.030	0.010
7			0.050	0.129	0.100	0.114	0.100	0.075	0.045	
8			0.015	0.050	0.080	0.075	0.065	0.030	0.015	
9			0.010	0.025	0.065	0.025	0.010	0.005	0	
10				0.040	0.030	0.040	0.050	0.020	0	
11				0.005	0.005	0.010	0.005	0.005	0.005	
12				0.010	0.005	0.015	0.005	0	0	
$N(t)$ Av		1.52	3.43	4.82	5.19	5.15	4.58	3.64	2.60	1.29
$N(t)$ Var		0.72	3.79	6.43	5.92	6.46	6.96	5.71	4.35	1.90
t (r.l.) $N \setminus$		$E_0=845$ MeV; $m=200$ showers; $\Delta E_0=65$ MeV								
		$\frac{1}{2}$	$1\frac{1}{2}$	$2\frac{1}{2}$	$3\frac{1}{2}$	$4\frac{1}{2}$	$5\frac{1}{2}$	$6\frac{1}{2}$	$7\frac{1}{2}$	$9\frac{1}{2}$
0		0.010	0.025	0.015	0.020	0.040	0.040	0.080	0.155	0.365
1		0.680	0.230	0.040	0.060	0.090	0.115	0.105	0.195	0.225
2		0.175	0.145	0.100	0.110	0.100	0.135	0.175	0.245	0.200
3		0.105	0.220	0.185	0.115	0.130	0.195	0.195	0.165	0.120
4		0.030	0.155	0.160	0.150	0.170	0.150	0.180	0.090	0.050
5			0.080	0.180	0.205	0.155	0.155	0.095	0.060	0.030
6			0.085	0.150	0.150	0.125	0.090	0.080	0.040	0
7			0.030	0.080	0.075	0.105	0.045	0.040	0.030	0.010
8			0.025	0.050	0.075	0.055	0.015	0.035	0.010	
9			0.005	0.020	0.010	0.025	0.035	0.010	0	
10				0.005	0.005	0	0.015	0.005	0.010	
11				0.005	0.020	0	0.005			
12				0.010	0.005	0	0			
13						0.005	0.005			
$N(t)$ Av		1.46	3.17	4.60	4.70	4.35	3.90	3.41	2.47	1.40
$N(t)$ Var		0.66	3.79	4.69	5.34	5.37	5.63	4.54	4.05	2.17
t (r.l.) $N \setminus$		$E_0=528$ MeV; $m=312$ showers; $\Delta E_0=58$ MeV								
		$\frac{1}{2}$	$1\frac{1}{2}$	$2\frac{1}{2}$	$3\frac{1}{2}$	$4\frac{1}{2}$	$5\frac{1}{2}$	$6\frac{1}{2}$	$7\frac{1}{2}$	$9\frac{1}{2}$
0		0.003	0.026	0.032	0.051	0.058	0.179	0.337	0.420	0.756
1		0.737	0.237	0.115	0.083	0.135	0.202	0.234	0.237	0.163
2		0.138	0.240	0.200	0.192	0.224	0.250	0.170	0.173	0.070
3		0.096	0.202	0.160	0.192	0.215	0.154	0.151	0.080	0.010
4		0.013	0.147	0.163	0.192	0.138	0.106	0.051	0.048	
5		0.010	0.086	0.157	0.128	0.109	0.067	0.029	0.026	
6		0.003	0.038	0.093	0.099	0.064	0.032	0.013	0.010	
7			0.019	0.058	0.048	0.032	0.006	0.013	0	
8			0	0.013	0.010	0.022	0	0.003	0.006	
9			0	0.006	0.003	0.003	0.003			
10			0	0.006						
11			0.003							
12										
$N(t)$ Av		1.42	2.75	3.61	3.49	3.14	2.19	1.57	1.25	0.33
$N(t)$ Var		0.70	2.71	3.99	3.47	3.60	2.90	2.65	2.25	0.42
t (r.l.) $N \setminus$		$E_0=277$ MeV; $m=300$ showers; $\Delta E_0=25$ MeV								
		$\frac{1}{2}$	$1\frac{1}{2}$	$2\frac{1}{2}$	$3\frac{1}{2}$	$4\frac{1}{2}$	$5\frac{1}{2}$	$6\frac{1}{2}$	$7\frac{1}{2}$	$9\frac{1}{2}$
0		0.023	0.057	0.090	0.187	0.357	0.507	0.603	0.663	0.833
1		0.717	0.307	0.260	0.213	0.240	0.253	0.170	0.207	0.117
2		0.143	0.240	0.267	0.293	0.230	0.133	0.160	0.100	0.047
3		0.090	0.223	0.177	0.140	0.110	0.070	0.047	0.030	0.003
4		0.017	0.097	0.113	0.103	0.043	0.030	0.007		
5		0.010	0.040	0.053	0.043	0.003	0.003	0.010		
6			0.030	0.023	0.013	0.017	0.003	0.003		
7			0.007	0.003	0.007					
8				0.007						
9				0.007						
10										
$N(t)$ Av		1.39	2.27	2.32	1.98	1.32	0.89	0.73	0.50	0.22
$N(t)$ Var		0.68	2.08	2.65	2.29	1.78	1.32	1.18	0.63	0.28

Only showers which could be clearly separated one from another were scanned. Each of the stereoscopic views was scanned separately and the number of tracks in each gap counted. If there was any inconsistency between the two views, the larger number of electrons was chosen because it is likely that a track might be obscured in one view but not in the other.

One of the largest difficulties in scanning came from trying to identify and disregard back-scattered electrons. It is estimated that approximately $\frac{1}{4}$ of all shower electrons seen within 60 deg are going backward. The inefficiencies in recognizing back-scattered electrons could systematically increase the average number of electrons observed by about 7%,³ but because this bias will always be present when this type of analysis is performed no correction has been made to the data.

In the high-energy showers, the number of electrons seen at the shower maximum tends to become rather large and the possibility of missing an electron, because it is obscured by other tracks, is not negligible. A crude estimate of this "saturation" is made by using

$$N = N_{\text{ob}} / (1 - N_{\text{ob}}R),$$

where N is the actual number of electrons present, N_{ob} is the observed number and R is the ratio of the area taken up by one track to the total average area over which the tracks in any gap are distributed. For the geometry of this experiment it is estimated that R is about 0.01. This value gives a 10% correction to the average number of electrons, if ten electrons are observed. It is clear that this correction could become very important if showers with energies of greater than 1 BeV were observed, or if small gap spacing and larger track widths were necessary, as in spark chambers. In the following results it will be indicated when the above "saturation" correction has been made to the data.

The possibility of missing low-energy showers because they might produce too few electrons is estimated to be very small. Background from anything but neighboring showers is negligible and contamination from adjacent showers will only tend to distort fluctuations and will not affect average numbers.

III. DEFINITIONS AND EXPERIMENTAL DATA

To determine the behavior of both the experimentally observed showers and Wilson's calculated showers, $N(t)$, the number of electrons occurring at various thicknesses, t (within 60 deg of the shower axis, for the experiment; or with energies greater than 10 or 8 MeV for the calculation) is measured for each individual shower.

³ This estimate is made by using the results of Refs. 1, 7, and 8 and Wilson's model (see Sec. V) to estimate that 27% of all electrons within 60 deg of the shower axis are moving backward. Though it is relatively easy to recognize electrons which cross a gap in the forward direction and then scatter backward, it is harder to identify back-scattered electrons which have come from forward moving photons. It is assumed that almost all electron-produced back-scatters will be recognized but only about one-half of the photon-produced back-scatters will be recognized. This leads to an approximate back-scattering efficiency of 75%.

TABLE II. Experimental results: the probability of observing N_{max} electrons at the shower maximum, and the probability of observing the shower maximum at thickness t_{max} for four values of primary energy. The average values and variances of N_{max} and t_{max} are given in the last rows.

(a)				
$N_{\text{max}} \backslash E_0$ (MeV)	990	845	528	277
0	0	0	0	0
1	0.005	0	0	0.023
2	0.015	0.005	0.003	0.137
3	0.005	0.025	0.080	0.317
4	0.015	0.025	0.183	0.273
5	0.055	0.110	0.253	0.137
6	0.129	0.195	0.231	0.083
7	0.244	0.225	0.170	0.017
8	0.184	0.225	0.054	0.007
9	0.119	0.095	0.016	0.007
10	0.159	0.040	0.006	
11	0.035	0.030	0.003	
12	0.035	0.015		
13		0.010		
N_{max} Av	7.80	7.17	5.50	3.75
Var	4.00	3.53	2.23	1.91

(b)				
t_{max} (r.l.) $\backslash E_0$ (MeV)	990	845	528	277
0	0	0	0	0.007
$\frac{1}{2}$	0.010	0	0.016	0.063
$1\frac{1}{2}$	0.055	0.085	0.086	0.287
$2\frac{1}{2}$	0.194	0.195	0.295	0.257
$3\frac{1}{2}$	0.219	0.235	0.215	0.210
$4\frac{1}{2}$	0.219	0.180	0.231	0.097
$5\frac{1}{2}$	0.154	0.150	0.080	0.057
$6\frac{1}{2}$	0.099	0.085	0.045	0.017
$7\frac{1}{2}$	0.035	0.050	0.032	0.003
$9\frac{1}{2}$	0.015	0.020		0.003
t_{max} Av	4.22	4.19	3.64	2.75
Var	2.79	3.12	2.24	2.14

From these numbers the following quantities are determined:

N_{max} , the maximum number of electrons observed in any of the gaps.

t_{max} , the thickness at which N_{max} is observed. (If the maximum occurs in more than one gap the arbitrary rule has been followed that if there are two equal peaks not in adjacent gaps the first is designated as the maximum, whereas if there are two equal peaks in adjacent gaps or three or more equal peaks, the second is chosen.)

N_{Σ} , the sum of the number of electrons at the peak and the number one r.l. to either side of the maximum. (If the peak occurs at 0 or $9\frac{1}{2}$ r.l. N_{Σ} is undefined.)

L_T , the track length of the shower (in r.l.) parallel to the shower axis. The following approximation was used:

$$L_T = \frac{1}{2}N\left(\frac{1}{2}\right) + \sum_{t=1}^6 N\left(t + \frac{1}{2}\right) + \frac{3}{2}[N(7\frac{1}{2}) + N(9\frac{1}{2})] \approx \int_0^{9\frac{1}{2}} N(t) dt.$$

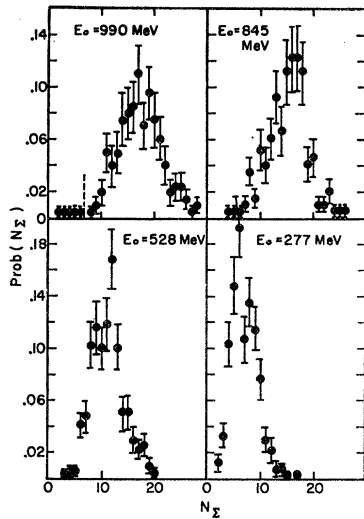


FIG. 1. The experimentally measured probability of observing N_{Σ} electrons in the three gaps around the shower maximum as a function of N_{Σ} , for the four primary energies considered. The dashed line shows the limit of the data discounted in Table III(b).

When computing N_{\max} and N_{Σ} from Wilson's data the "gaps" are assumed to be at the same thicknesses as in the experiment.

Showers within a given primary energy interval are combined and the probability of observing a particular number for each of the above quantities is computed, as well as the averages (indicated by $\langle \rangle$) and variances of these numbers. When computing $\langle L_T \rangle$ from Crawford and Messel's or Wilson's calculations a numerical integration $\int_0^{\infty} \langle N(t) \rangle dt$ has been carried out in which the contribution of the exponentially decaying shower tail has been included.

The uncorrected experimental results are given in Tables I through III and Figs. 1 and 2 as functions of

TABLE III. Experimental results: (a) the average values and variances of the track length, L_T (in r.l.), and of N_{Σ} . Probability distributions are given in Figs. 1 and 2. Experimental results: (b) Experimental results corrected by omission of a small number of events which differ widely from the main body of the data. (See text and Figs. 1 and 2.)

(a)				
E_0 (MeV)	990	845	528	277
L_T Av	33.4	30.6	20.3	11.8
Var	55.3	45.1	19.5	14.8
N_{Σ} Av	17.0	15.1	11.1	6.98
Var	20.8	14.5	9.53	6.10
(b)				
E_0 (MeV)	990	845	528	277
L_T Av	34.4	30.7	20.3	11.8
Var	30.7	37.0	19.5	14.8
N_{Σ} Av	17.2	15.1	11.1	6.98
Var	18.0	14.5	9.5	6.10

E_0 . The probability of observing N electrons at a given thickness and the average number observed at each thickness are given in Table I. The average number of electrons observed in the last gap is anomalously low, especially for the 528-MeV run. These low values are probably caused by poor chamber conditions and illumination rather than any real effect like the absence of back scattering.

Table II gives the average number of electrons at the shower maximum, $\langle N_{\max} \rangle$, and the probability of finding a given number of electrons at the maximum. It also lists the probability of finding the maximum at a particular depth, t_{\max} .

Table III(a) gives the average values of the track length L_T and of N_{Σ} . The probability distributions of these two quantities are shown in Figs. 1 and 2. The general shape of these distributions (and also the distributions of N_{\max}) can be approximated by Gaussians. However, in the two high-energy runs there are several events which differ radically from the main body of the data. If these events are used in calculating the variances, Gaussians with the same variance do not agree at all well with the data. It is felt that whether or not these events are background,⁴ they give a misleading impression of the magnitude of the fluctuations. Table III(b) gives the averages and variances of L_T and N_{Σ} leaving out these widely fluctuating events, which fall to the left of the dotted lines on Figs. 1 and 2.

Figure 3 shows interpolated "transition curves," i.e., $\langle N(t) \rangle$ as a function of t , for showers with primary electrons of 300, 500, 700, and 1000 MeV. These curves have been obtained from smooth fits to the experimental values of $\langle N(t) \rangle$ versus energy with t the parameter.

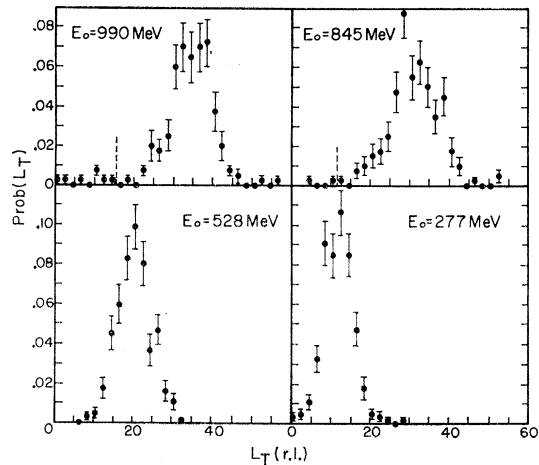


FIG. 2. The experimentally measured probability per radiation length of observing a given track length L_T as a function of L_T . The dashed lines show the limit of the data discounted in Table III(b).

⁴ It is quite possible that these events are due to low-energy electrons produced in the air between the analyzing magnet poles.

TABLE IV. Wilson's Monte Carlo results for primary electrons of 50-, 100-, 200-, and 300-MeV energy. The total number of shower histories analyzed; the average number and the variance of electrons with $E \geq 10$ MeV; and the average number of electrons with $E \geq 8$ MeV, as functions of thickness.

t (r.l.)	$\frac{1}{2}$	1	$1\frac{1}{2}$	2	$2\frac{1}{2}$	3	$3\frac{1}{2}$	4	$4\frac{1}{2}$	5	$5\frac{1}{2}$	6	$6\frac{1}{2}$	7	$7\frac{1}{2}$	8	$8\frac{1}{2}$	9
50-MeV primary electron; number of showers = 198																		
$\langle N \rangle$ ($E \geq 10$ MeV)	0.94	0.75	0.37	0.21	0.05	0.11	0.05	0.05	0.02	0.01								
Var ($E \geq 10$ MeV)	0.09	0.21	0.24	0.22	0.05	0.14	0.05	0.05	0.02	0.01								
$\langle N \rangle$ ($E \geq 8$ MeV)	0.97	0.84	0.48	0.27	0.09	0.14	0.08	0.07	0.02	0.01								
100-MeV primary electron; number of showers = 100																		
$\langle N \rangle$ ($E \geq 10$ MeV)	1.03	1.09	0.97	0.71	0.33	0.34	0.28	0.25	0.15	0.08	0.04	0.09	0.05	0.05	0.01	0.04	0.02	0.01
Var ($E \geq 10$ MeV)	0.17	0.44	0.38	0.41	0.28	0.38	0.30	0.31	0.15	0.09	0.04	0.08	0.05	0.05	0.01	0.06	0.02	0.01
$\langle N \rangle$ ($E \geq 8$ MeV)	1.04	1.18	1.07	0.94	0.51	0.42	0.35	0.30	0.22	0.12	0.07	0.13	0.09	0.07	0.03	0.06	0.05	0.01
200-MeV primary electron; number of showers = 98																		
$\langle N \rangle$ ($E \geq 10$ MeV)	1.22	1.57	1.43	1.37	1.01	0.80	0.71	0.72	0.49	0.46	0.29	0.41	0.17	0.25	0.11	0.13	0.05	0.07
Var ($E \geq 10$ MeV)	0.37	1.27	0.95	1.04	0.98	0.75	0.63	0.79	0.45	0.53	0.35	0.61	0.18	0.25	0.10	0.17	0.07	0.07
$\langle N \rangle$ ($E \geq 8$ MeV)	1.24	1.67	1.63	1.66	1.17	1.06	0.84	0.96	0.67	0.51	0.40	0.49	0.23	0.31	0.15	0.15	0.08	0.10
300 MeV primary electron; number of showers = 100																		
$\langle N \rangle$ ($E \geq 10$ MeV)	1.14	1.57	1.87	2.23	1.94	1.67	1.32	1.22	0.75	0.84	0.50	0.54	0.36	0.44	0.20	0.27	0.17	0.22
Var ($E \geq 10$ MeV)	0.22	0.77	0.80	1.73	1.62	1.36	1.22	1.25	0.77	0.97	0.51	0.65	0.41	0.33	0.26	0.46	0.26	0.28
$\langle N \rangle$ ($E \geq 8$ MeV)	1.15	1.66	2.06	2.44	2.24	2.05	1.60	1.50	0.95	0.95	0.62	0.65	0.47	0.50	0.30	0.31	0.21	0.22

TABLE V. Wilson's Monte Carlo results for primary photons of 50-, 100-, 200-, and 300-MeV energy.

t (r.l.)	$\frac{1}{2}$	1	$1\frac{1}{2}$	2	$2\frac{1}{2}$	3	$3\frac{1}{2}$	4	$4\frac{1}{2}$	5	$5\frac{1}{2}$	6	$6\frac{1}{2}$	7	$7\frac{1}{2}$	8	$8\frac{1}{2}$	9
50-MeV primary photon; number of showers = 100																		
$\langle N \rangle$ ($E \geq 10$ MeV)	0.19	0.46	0.39	0.29	0.22	0.27	0.21	0.15	0.10	0.13	0.06	0.03	0.03	0.01	0			
Var ($E \geq 10$ MeV)	0.23	0.57	0.34	0.33	0.25	0.26	0.25	0.15	0.13	0.17	0.06	0.02	0.05	0.01	0			
$\langle N \rangle$ ($E \geq 8$ MeV)	0.23	0.48	0.45	0.41	0.25	0.34	0.25	0.17	0.15	0.16	0.10	0.07	0.04	0.03	0.02			
100-MeV primary photon; number of showers = 100																		
$\langle N \rangle$ ($E \geq 10$ MeV)	0.47	0.80	0.66	0.71	0.56	0.52	0.38	0.38	0.34	0.28	0.16	0.23	0.09	0.12	0.07	0.04	0.03	0.03
Var ($E \geq 10$ MeV)	0.77	0.80	0.60	0.63	0.49	0.53	0.42	0.48	0.42	0.32	0.21	0.18	0.10	0.17	0.10	0.04	0.05	0.03
$\langle N \rangle$ ($E \geq 8$ MeV)	0.47	0.86	0.77	0.83	0.64	0.67	0.42	0.43	0.39	0.37	0.24	0.29	0.16	0.13	0.19	0.04	0.04	0.05
200-MeV primary photon; number of showers = 100																		
$\langle N \rangle$ ($E \geq 10$ MeV)	0.92	1.19	1.18	1.20	1.06	0.97	0.73	0.70	0.63	0.61	0.42	0.42	0.31	0.32	0.23	0.14	0.09	0.10
Var ($E \geq 10$ MeV)	1.15	1.45	0.98	1.04	0.88	0.87	0.76	0.59	0.61	0.70	0.42	0.46	0.33	0.46	0.30	0.14	0.12	0.15
$\langle N \rangle$ ($E \geq 8$ MeV)	0.93	1.26	1.25	1.37	1.23	1.14	0.87	0.85	0.75	0.71	0.54	0.55	0.40	0.40	0.24	0.24	0.11	0.16
300-MeV primary photon; number of showers = 100																		
$\langle N \rangle$ ($E \geq 10$ MeV)	0.71	1.25	1.43	1.75	1.74	1.85	1.43	1.31	1.04	1.08	0.66	0.73	0.48	0.55	0.40	0.47	0.27	0.30
Var ($E \geq 10$ MeV)	1.01	1.85	1.70	2.01	1.53	1.85	1.64	1.66	0.98	1.27	0.80	0.74	0.57	0.85	0.46	0.67	0.40	0.43
$\langle N \rangle$ ($E \geq 8$ MeV)	0.71	1.31	1.54	1.97	1.91	2.08	1.63	1.45	1.23	1.24	0.82	0.89	0.58	0.63	0.48	0.57	0.40	0.35

IV. WILSON'S MONTE CARLO CALCULATIONS

The following is a summary of the shower histories calculated by Wilson¹ in 1952. The axes given in Figs. 4, 7, and 8 of his article apparently were incorrectly labeled.⁵

Tables IV and V give numbers of secondary electrons calculated as a function of thickness for primary electrons and photons having energies of 50, 100, 200, and 300 MeV. $\langle N(t) \rangle$ and the variances of $N(t)$ are calculated for electrons with energies ≥ 10 MeV. $\langle N(t) \rangle$ is also given for electrons with energies ≥ 8 MeV (not including the number of electrons with energies ≥ 8 MeV produced by photons with energies < 10 MeV).

Transition curves of $\langle N(t) \rangle$ given in Tables IV and V compare well with the recent results of Crawford and

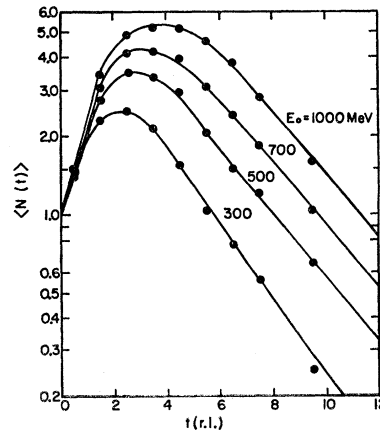


Fig. 3. The transition curves of the average shower development for primary energies $E_0 = 300, 500, 700, 1000$ MeV. These average numbers of electrons as a function of distance in lead have been interpolated from the experimental data.

⁵ Inconsistency of the published results with the histories was first noted by P. A. Bender, M. A. thesis, Washington University, St. Louis Missouri, 1955 (unpublished).

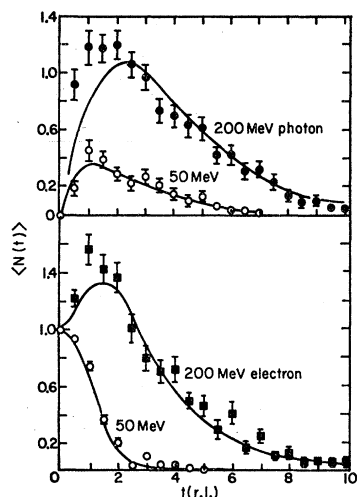


FIG. 4. A comparison of the average number of electrons with energies $E \geq 10$ MeV as a function of depth, as given by the Monte Carlo calculations of Crawford and Messel (smooth curves) with the results obtained by R. R. Wilson (points with statistical errors shown). The comparison is given for primary electrons and photons of 200- and 50-MeV energy.

Messel.² Figure 4 shows a comparison between these two Monte Carlo calculations for primary electrons and photons of 50 and 200 MeV. Though the statistics of Wilson's curves are poor, there is a tendency for Wilson's values to be slightly larger than those of Crawford and Messel. The anomalously fast rise of Wilson's 200-MeV photon shower curve is probably a statistical fluctuation.

Other results from Wilson's calculations are shown in Figs. 5, 6, and 7. In Figs. 6 and 7 where there is an overlap in the information furnished by Wilson and by Crawford and Messel, the results of Crawford and Messel have been used because of their better statistical accuracy.

V. COMPARISON OF EXPERIMENT AND CALCULATION

The experimentally measured transition curves can be compared approximately with the Monte Carlo cal-

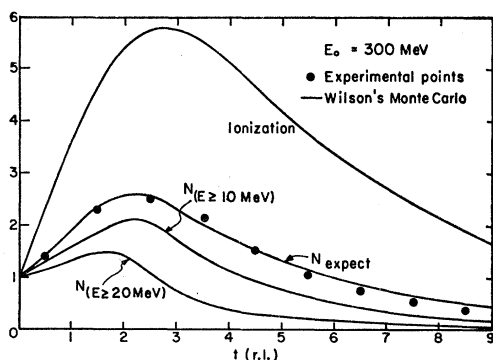


FIG. 5. A comparison of the Monte Carlo transition curves of Wilson with the experimentally measured curves as given in Fig. 3, (for 300-MeV primary electrons). The ordinate plotted corresponds to the quantities labeled on each curve. From Wilson's data they are: the total ionization normalized to the ionization loss (7.5 MeV) of one electron per r.l.; $N(t)_{(E \geq 10 \text{ MeV})}$, the average number of electrons with energies greater than 10 MeV; $N(t)_{(E \geq 20 \text{ MeV})}$, the average number of electrons with energies greater than 20 MeV; $N(t)_{\text{expect}}$, the average number of electrons expected to be comparable with the experimental results (see text). The experimental transition curve is indicated by circular points.

culations if the angular cutoff of the experiment is related to the energy cutoff of the calculation. The comparison cannot be very accurate, however, because of the large fraction of low-energy electrons in the showers, and the fact that scattering angle is not uniquely determined by an electron's energy. The following discussion uses an argument of Wilson¹ which assumes that shower electrons move straight forward along the shower axis until they reach a certain energy E , at which point they begin to move randomly in the lead. Thus, according to his model the number of electrons observed within 60 deg of the shower axis is the number with energies greater than E , plus a fraction of the number with energies less than E . A further correction should be made because not all the electrons with energies above E will really have directions within 60 deg of the shower axis.

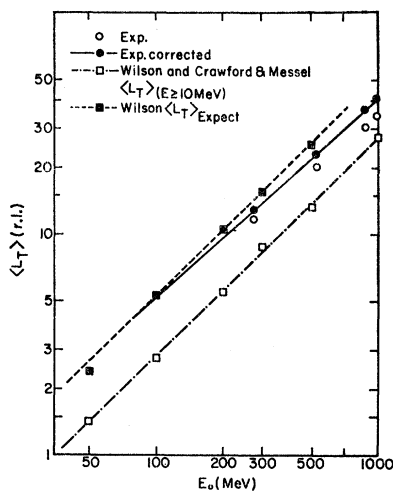


FIG. 6. The average track length $\langle L_T \rangle$ as a function of primary energy. Shown as labeled are: the uncorrected experimental track length; the experimental $\langle L_T \rangle$ corrected for "saturation" and the "tail integral"; the track length calculated by Wilson and by Crawford and Messel for secondary energies $E \geq 10$ MeV; the track length calculated by Wilson for electrons with energies $E \geq 8$ MeV plus the track length of electrons with energies $E \leq 8$ MeV which would have directions within 60 deg of the shower axis (labeled $\langle L_T \rangle_{\text{expect}}$). Lines give approximate fit to points.

Roberg and Nordheim⁶ give accurate calculations of the rms scattering angle of shower electrons as a function of energy. They show that the onset of random motion of electrons, as indicated by an rms scattering angle of about 1 rad, corresponds to an energy E of about 10 MeV for lead.

In his original paper, Wilson gave transition curves for total ionization, in units of energy lost by an electron in passing through one r.l., or 7.5 MeV. $\langle N(t) \rangle$ as given in Sec. IV for electrons with energies above 10 MeV, is equal to the ionization of these electrons (in the units defined above), because the latter are assumed to be

⁶ J. Roberg and L. W. Nordheim, Phys. Rev. 75, 444 (1949).

traveling parallel to the shower axis. The difference between the total ionization $I(t)$ and the number of electrons with energies greater than 10 MeV, $N(t)$ gives the total ionization of electrons with energies below 10 MeV. Because the low energy electrons are assumed to be moving randomly in the lead it is easy to calculate the number of low energy electrons, which are moving forward within 60 deg of the shower axis in the air gap between lead plates.

Namely

$$\begin{aligned} \Delta N_f &= \int_0^{60^\circ} \frac{1}{2}(I-N) \cos\theta \sin\theta d\theta, \\ &= 0.187(I-N) = 0.187\Delta I, \end{aligned}$$

where $\frac{1}{2}(I-N)$ is the ionization produced by electrons with energies less than 10 MeV moving in the forward direction and θ is the angle relative to the shower axis, at which electrons emerge from the lead plates.

The number of electrons with energies greater than 10 MeV which would travel at an angle greater than 60 deg to the axis can be estimated from the energy distribution of secondary electrons given by Richards and Nordheim,⁷ and from the mean square scattering angle of these electrons given by Roberg and Nordheim.⁶ Very few electrons with energies greater than 20 MeV will be scattered outside of 60 deg. About 20% of the electrons with energies between 10 and 20 MeV will be outside 60 deg.

Using Wilson's data and the above assumptions the average number of electrons within 60° of the shower axis, expected from the Monte Carlo calculations, is

$$\begin{aligned} N(t)_{\text{expect}} &= N(t)_{(E \geq 10 \text{ MeV})} \\ &\quad + 0.19\Delta I(t) - 0.20\Delta N(t)_{(20 > E > 10 \text{ MeV})}. \end{aligned}$$

Figure 5 shows the relative sizes of the above quantities for 300-MeV showers. The excellent agreement, for 300-MeV electron-initiated showers, between the calculated curve and the experimental results taken from Fig. 3, must be partly fortuitous. It should be stressed that the comparison is more approximate than the agreement of the curves would seem to indicate for no corrections have been made for scanning efficiencies, saturation or back scattering, and the derivation of $N(t)_{\text{expect}}$ does not pretend to be exact.

The number of electrons in the tail of the shower should go as $e^{-\sigma_\gamma t}$, where σ_γ is the total absorption coefficient per radiation length for photons. The exponential tails of the experimental showers are in good agreement with those expected from the calculation. The experimental data give $\sigma_\gamma = 0.30 \pm 0.02 \text{ r.l.}^{-1}$ for the average of all primary energies. Wilson's "expected" curves for 300 and 500 MeV give $\sigma_\gamma = 0.28 \text{ r.l.}^{-1}$. At large thickness, σ_γ should tend toward 0.24 r.l.^{-1} , which is the

⁷ J. A. Richards and L. W. Nordheim, Phys. Rev. **74**, 1106 (1948).

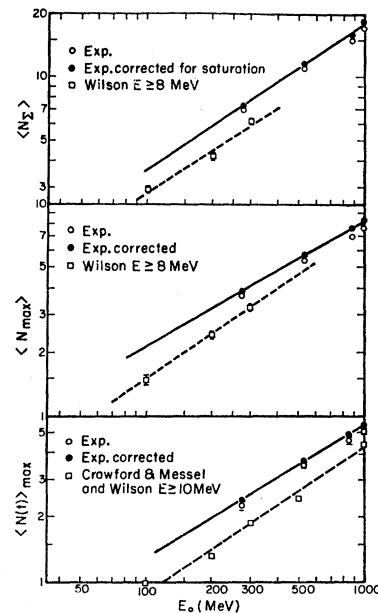


FIG. 7. The values of $\langle N_\Sigma \rangle$, $\langle N_{\text{max}} \rangle$, and $\langle N(t)_{\text{max}} \rangle$ as a function of energy. Shown are the experimental data, the experimental data corrected for saturation, and the calculations of Wilson and of Crawford and Messel for all electrons with energies greater than E . Lines give approximate fits to points.

minimum photon cross section; but the data of Blocker *et al.*⁸ show that this minimum absorption is not attained until a shower depth of 15 r.l., even for total ionization observations.

VI. AVERAGE BEHAVIOR OF SHOWERS

The experimentally observed track lengths are plotted in Fig. 6 as a function of primary energy. Also shown are the track lengths after correction for saturation and for the integral of the shower tail which is not observed in the chamber. This tail correction is just $\Delta L_T = N(t = 9\frac{1}{2})/\sigma_\gamma$, where $\sigma_\gamma = 0.30$ per radiation length.

Figure 6 also shows results obtained from the calculations of Crawford and Messel and of Wilson. The points labeled $\langle L_T \rangle_{(E \geq 10 \text{ MeV})}$ give the track length parallel to the shower axis for electrons with energies greater than 10 MeV. $\langle L_T \rangle_{(\text{expect})}$ is obtained from Wilson's data by adding the track length of electrons with energies greater than 8 MeV to the computed longitudinal track length of electrons below 8 MeV within 60 deg of the axis. This sum should be approximately comparable with the experimental results.

The corrected experimental data fit an equation of the form $\langle L_T \rangle = CE_0^x$ with $C = 0.073 \text{ r.l.}$, $x = 0.92$, and E_0 measured in MeV. One would normally expect a linear variation of track length with energy, and both sets of Monte Carlo results have approximately linear behavior. Though the nonlinear behavior of the experimental results may not be statistically very significant, it is interesting that Hazen⁹ has also observed this behavior (with poor statistics) in copper.

⁸ W. Blocker, R. Kenney, and W. Panofsky, Phys. Rev. **79**, 419 (1950).

⁹ W. E. Hazen, Phys. Rev. **99**, 911 (1955).

TABLE VI. A comparison of the constant $K(E_0) = L_T/E_0$ (r.l./MeV) derived from experimental data, Monte Carlo calculations, and theoretical calculations, E is the minimum energy of electrons counted.

	K independent of E_0	K (E_0) E_0 (MeV)						
		50	100	200	300	500	700	1000
Experimental data uncorrected (Fig. 6)					0.041	0.039	0.037	0.035
Experimental data corrected (Fig. 6)					0.047	0.045	0.044	0.043
Monte Carlo, Wilson, $\langle L_T \rangle_{\text{expect}}$ (Fig. 6)		0.048	0.053	0.053	0.052	0.051		
Monte Carlo, Crawford and Messel, $E \geq 10$ MeV ^a		0.029	0.028	0.028		0.027		0.028
Monte Carlo, Crawford and Messel, total L_T ^b		0.034	0.032	0.032		0.032		0.032
Experimental data, Hazan ^c (9 showers)	0.040							
Calculation, Richards and Nordheim, $E \geq 10$ MeV ^d	0.034							

^a Reference 2 and Fig. 6 a numerical integration of $N(t)$.
^b Reference 2 the total track length: not just the component parallel to the shower axis.
^c Reference 9 measured in a combination lead and carbon chamber.
^d Reference 7 calculated for lead.

The present data can be most easily compared with results of previous measurements and calculations by evaluating the ratio $K(E_0) = \langle L_T \rangle / E_0$; values of this ratio are listed in Table VI.

Empirical expressions of the form CE_0^x also can be fitted to the other characteristic shower quantities. Values of C and x for the experimental data on $\langle N_\Sigma \rangle$, $\langle N_{\text{max}} \rangle$, and $\langle N(t) \rangle_{\text{max}}$ (the peak of the transition curve) are given in Table VII. Figure 7 shows these quantities as function of primary energy, and also gives the results of the calculations of Wilson, and of Crawford and Messel, for comparison. These calculated values do not include contributions from low energy, randomly moving electrons, which would only increase the value of the coefficient C , making it agree with the experimental value, without changing the exponent x .

It is significant that the number of electrons at the shower maximum, $\langle N(t) \rangle_{\text{max}}$, does not increase as fast with primary energy as predicted by shower theory¹⁰ (approximation A , B , etc.). Thus on the one hand it appears dangerous to use the analytic form $E_0 [\ln(E_0/a)]^{-1/2}$, to extrapolate the data to higher energies; on the other hand, this experiment gives no evidence that the exponent x will remain constant as the primary energy is increased.

VII. FLUCTUATIONS

The experimental probability distributions of the number of electrons at a given thickness of lead can be

TABLE VII. The experimentally determined constants C and x in the equations of the form $n = CE_0^x$, where the quantities $\langle L_T \rangle$, $\langle N_\Sigma \rangle$, $\langle N_{\text{max}} \rangle$, and $\langle N(t) \rangle_{\text{max}}$ are substituted for n and E_0 is the primary energy in MeV.

n	C (r.l.)	x
$\langle L_T \rangle$	0.073	0.92
$\langle N_\Sigma \rangle$	0.143	0.70
$\langle N_{\text{max}} \rangle$	0.143	0.59
$\langle N(t) \rangle_{\text{max}}$	0.076	0.62

¹⁰ See, for instance, B. Rossi and K. Greisen, Rev. Mod. Phys. 13, 24 (1941).

TABLE VIII. Corrected experimental data: (a) Inherent fluctuations in L_T , N_Σ , and N_{max} : the variance and its estimated error after fluctuations caused by primary energy resolutions have been subtracted; and the relative standard error (Var corrected)^{1/2}/ $n = dn/n$ for $n = L_T, N_\Sigma, N_{\text{max}}$. (b) The expected standard error in primary energy evaluation from measuring the value of $n(L_T, N_\Sigma, \text{ or } N_{\text{max}})$ for a single shower, where $n = CE^x$ and $dE_0/E_0 = x^{-1}dn/n$.

(a)			
L_T E_0 (MeV)	Var corrected	$[\text{Var (corrected)}]^{1/2}/L_T$	
990	24.5±5.5	0.14±0.02	
845	33.0±4.5	0.19±0.02	
528	15.1±2.0	0.19±0.01	
277	14.0±1.5	0.32±0.02	
N_Σ E_0		$[\text{Var (corrected)}]^{1/2}/N_\Sigma$	
990	14.7±2.0	0.22±0.02	
845	11.9±1.5	0.23±0.01	
528	6.9±1.0	0.24±0.01	
277	5.5±0.6	0.34±0.01	
N_{max} E_0		$[\text{Var (corrected)}]^{1/2}/N_{\text{max}}$	
990	3.4±0.40	0.24±0.01	
845	3.0±0.35	0.24±0.01	
528	1.6±0.22	0.23±0.01	
277	1.7±0.19	0.35±0.02	
(b)			
	x	$E_0 = 300$ MeV dn/n dE_0/E_0	$E_0 = 500$ MeV—1 BeV dn/n dE_0/E_0
L_T	0.92	±0.32 ±0.35	±0.18 ±0.20
N_Σ	0.72	±0.34 ±0.47	±0.23 ±0.32
N_{max}	0.61	±0.35 ±0.57	±0.24 ±0.39

approximated by Poisson or Polya distributions which use the experimentally measured mean values and variances of $N(t)$. The Polya b parameter varies with absorber thickness in a manner similar to that predicted by Messel.¹¹

The probability distributions of L_T , N_Σ , and N_{max} can be fitted with Gaussians as noted in Sec. III. Some of the width of these distributions is caused by the en-

¹¹ H. Messel, Proc. Phys. Soc. (London) A64, 807 (1951).

ergy dispersion of the primary electrons. If the spread in primary energy is taken into account the inherent dispersion can be found for the various shower quantities. The results are listed in Table VIII(a). It is interesting to estimate the statistical accuracy within which the energy of one shower may be evaluated by observing such features as L_T , N_Σ , or N_{\max} . In Sec. 6 the average values of these quantities were found to have the behavior $n = CE_0^x$ hence $dE_0/E_0 = x^{-1} dn/n$. The expected standard errors, dE_0/E_0 , are listed in Table VII(b) for energies inferred from L_T , N_Σ , and N_{\max} . As might be expected, the use of N_Σ has some advantage in

statistical precision over N_{\max} and has the advantage over use of L_T , that N_Σ can be observed even at rather high energies with a chamber of modest dimensions.

ACKNOWLEDGMENTS

It is a pleasure to thank Professor Kenneth Greisen for many discussions and suggestions. I would also like to thank Professor R. R. Wilson for the use of his shower "histories" and Dr. E. Malamud and Dr. R. Schectman for their assistance in making these measurements.

PHYSICAL REVIEW

VOLUME 136, NUMBER 2B

26 OCTOBER 1964

Parity and Sign of the $\Sigma^+ \rightarrow n + \pi^+$ Decay Amplitude and a Model for π^+ Emission in Hypernuclear Decays*

FRANK VON HIPPEL†

The Enrico Fermi Institute for Nuclear Studies, The University of Chicago, Chicago, Illinois

(Received 8 June 1964)

It is found that the π^+/π^- emission ratio of 0.029 ± 0.01 in ΛHe^4 can be understood as due to the combined mechanisms: decay of a virtual Σ^+ hypernuclear state and the charge exchange of a π^0 from neutral Λ decay. Improvements upon simple perturbation-calculational techniques give $\pi^+/\pi^- \approx 0.015$ in near agreement with experiment, however, only if the decay $\Sigma^+ \rightarrow n + \pi^+$ is assumed to go to a final relative S state of the π^+ and neutron. Best agreement with experiment, for a D/F ratio of about 3 in the unitary symmetric strong pseudoscalar couplings, is obtained if the relative phases of the weak-decay amplitudes are determined according to unitary symmetry arguments. The observed low energy of the emitted π^+ mesons relative to the π^- mesons and the relative π^+ decay rates of different hypernuclei are qualitatively understood as primarily due to Pauli suppression effects in the final state. Reasons are given which suggest that the mesonic corrections to impulse-approximation calculations of the π^- and π^0 emission rates for the light hypernuclei will be small.

I. INTRODUCTION

WE consider here the simplest mechanisms which might account for the observed decay¹⁻⁷

$$\Lambda\text{He}^4 \rightarrow (\text{nucleons}) + \pi^+ \quad (1.1)$$

and calculate the branching ratio of this mode (experimentally estimated⁶ at about 0.029 ± 0.01) relative to

the mode

$$\Lambda\text{He}^4 \rightarrow (\text{nucleons}) + \pi^- \quad (1.2)$$

for various assumptions concerning the strong and weak baryon-pion couplings. Our major result is that the observed rate for the decay (1.1) can be explained as due to constructive interference between the two processes represented in Fig. 1 which give $\pi^+/\pi^- \approx 0.015$. The constructive interference is compatible with the relative phases of the nonleptonic decay interactions obtained by Lee⁸ in fitting the experimental data to a

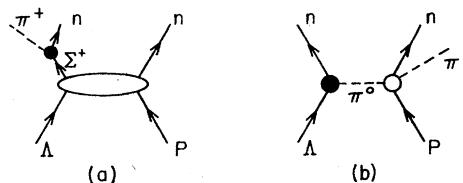


FIG. 1. Contributions found most important: (a) S -wave decay of a virtual Σ^+ state; (b) charge exchange on a proton of a π^0 from Λ decay.

* This work is supported by the U. S. Atomic Energy Commission

† Present address: Laboratory for Nuclear Science, Cornell University, Ithaca, New York.

¹ Y. W. Kang, N. Kwak, J. Schneps, and P. A. Smith, *Nuovo Cimento* **22**, 1297 (1961).

² A. Z. M. Ismail, I. R. Kenyon, A. W. Key, S. Lokanathan, and Y. Prakash, *Phys. Letters* **1**, 199 (1962).

³ S. N. Ganguli, N. K. Rao, and M. S. Swami, *Nuovo Cimento* **28**, 1258 (1963).

⁴ P. Allen, Sr., M. Heeran, and A. Montwill, *Phys. Letters* **3**, 274 (1963).

⁵ P. H. Steinberg and R. J. Prem, *Phys. Rev. Letters* **11**, 429 (1963).

⁶ M. J. Beniston, R. Levi-Setti, W. Püschel, and M. Raymund, *Phys. Rev.* **134**, B641 (1964).

⁷ M. M. Block, R. Gessaroli, S. Ratti, L. Grimellini, T. Kikuchi, L. Lendinara, L. Monari, and E. Harth, *Nuovo Cimento* **28**, 299 (1963).

⁸ B. W. Lee, *Phys. Rev. Letters* **12**, 83 (1964).